The Journal of Immunology

Fine-Tuning of Regulatory T Cell Function: The Role of Calcium Signals and Naive Regulatory T Cells for Regulatory T Cell Deficiency in Multiple Sclerosis

Alexander Schwarz, Marijana Schumacher, Daniel Pfaff, Kai Schumacher, Sven Jarius, Bettina Balint, Heinz Wiendl, Jürgen Haas and Brigitte Wildemann

J Immunol published online 10 April 2013
http://www.jimmunol.org/content/early/2013/04/09/jimmunol.1203224

The Journal of Immunology is published twice each month by The American Association of Immunologists, Inc., 1451 Rockville Pike, Suite 650, Rockville, MD 20852

Print ISSN: 0022-1767 Online ISSN: 1550-6606.

Published April 10, 2013, doi:10.4049/jimmunol.1203224

Fine-Tuning of Regulatory T Cell Function: The Role of Calcium Signals and Naive Regulatory T Cells for Regulatory T Cell Deficiency in Multiple Sclerosis

Alexander Schwarz,* Marijana Schumacher,* Daniel Pfaff,* Kai Schumacher,* Sven Jarius,* Bettina Balint,* Heinz Wiendl,† Jürgen Haas,* and Brigitte Wildemann*

The suppressor function of regulatory T cells (Tregs) is impaired in multiple sclerosis (MS), but the mechanisms underlying this deficiency are not fully understood. As Tregs counteract the sustained elevation of intracellular calcium, which is indispensable for full activation of conventional T cells (Tcons), we hypothesized that interference with this pathway might prompt MS-related Treg dysfunction. Using single-cell live imaging, we observed that Tregs rapidly reduce Ca^{2+} influx and downstream signals in Tcons upon cell contact, yet differ in their potency to efficiently suppress several target cells at the same time. Strikingly, individual Tregs harboring a $CD4^+CD25^+FOXP3^+CD45RA^+$ naive phenotype suppressed significantly more adjacent Tcons than did $CD4^+CD25^+FOXP3^+CD45RA^-$ memory Tregs. Some constituents even completely failed to dampen Tcon Ca^{2+} influx and were contained exclusively in the memory subset. In accordance with their more powerful suppressive performance, the Ca^{2+} signature was considerably enhanced in naive Tregs in response to TCR triggering, compared with the memory counterparts. MS Tregs displayed a significantly diminished suppression of mean Ca^{2+} influx in the sum of individual Tcons recorded. This reduced inhibitory activity was closely linked to decreased numbers of individual Tcons becoming suppressed by adjacent Tregs and, in turn, correlated with a marked reduction of naive subtypes and concomitant expansion of nonsuppressive memory phenotypes. We conclude that the superior achievement of naive Tregs is pivotal in maintaining Treg efficiency. As a consequence, MS Tregs become defective because they lack naive subtypes and are disproportionately enriched in memory cells that have lost their inherent downregulatory activity. ***The Journal of Immunology*****, 2013, 190: 000–000.**

$CD4^+CD25^+FOXP3^+$ regulatory T cells (Tregs) are key players in maintaining immunological self-tolerance, and a functional Treg deficiency is associated with various autoimmune diseases, including multiple sclerosis (MS) (1, 2). The ability of Tregs derived from patients with MS to downregulate both proliferation and cytokine secretion of activated conventional T cells (Tcons) in vitro is impaired, and this dysfunctional state is linked to a possibly thymic-dependent imbalance between naive and more short-lived memory cells that compose the peripheral Treg population (3–5). In addition, other abnormalities in Tregs that constitute functionally heterogeneous subsets are likely to contribute to the Treg defect in MS (6). Thus, recent findings demonstrate that less suppressive Tregs capable of producing IFN-γ are significantly increased in the peripheral blood of patients with MS (7) and that certain subtypes of patient-derived memory Tregs exhibit a downscaled suppressive performance in response to distinct T cell–activating stimuli (8). Notably, the defective Treg state is ameliorated under disease-modifying treatment, indicating that pharmacological modulation of Tregs might prove to be a promising strategy for restoring immunological homeostasis in MS (7, 9, 10). Although the molecular mechanisms that confer inhibition and reconstitution have been poorly understood, insights from an elegant, recently published study have provided compelling evidence that Tregs counteract the sustained elevation of intracellular free Ca^{2+} ions in target cells and thus interfere with a fundamental requirement for almost all aspects of Tcon activation (11). In that study, cocultured cell populations were used to demonstrate rapid suppression of Tcon Ca^{2+} signaling by Tregs, followed by downregulation of the Ca^{2+}-dependent transcription factor NFAT1 and NF-κB as important downstream events. However, using this approach, the authors could not elucidate in detail how Tregs interact with individual surrounding Tcons, and it remains unknown whether cells composing the Treg subset differ in their overall or individual ability to suppress Ca^{2+} influx in target cells.

In this article, we hypothesized that a difference in the ability to downregulate Ca^{2+} influx in effector T cells might affect the suppressive performance of total Tregs and might be involved in the Treg defect that can be detected in patients with MS. We established an in-house, single-cell live imaging assay by which we could directly monitor Ca^{2+} signatures in a multitude of individual cells exhibiting either a $CD4^+CD25^+FOXP3^+$ Treg or a $CD4^+CD25^-FOXP3^-$ Tcon phenotype and closely monitor the contact-dependent impact of a single Treg on Ca^{2+} signaling in one or more adjacent Tcons. Because we and others have shown

*Division of Molecular Neuroimmunology, Department of Neurology, University Hospital Heidelberg, 69120 Heidelberg, Germany; and †Department of Neurology, University Hospital Munster, 48149 Munster, Germany

Received for publication November 21, 2012. Accepted for publication March 7, 2013.

This work was supported by the Gemeinnützige Hertie-Stiftung (1.01.1/08/015) (to A.S.); the Young Investigator Award from the Faculty of Medicine, University of Heidelberg (to A.S.); the German Federal Ministry of Education and Research (Research Alliance "Understand MS" AII, FKZ 01GI0905–0913a) (to B.W.), and Center Research Grant 128 Multiple Sclerosis, Project A9 (to H.W.).

Address correspondence and reprint requests to Dr. Brigitte Wildemann, Division of Molecular Neuroimmunology, Department of Neurology, University Hospital Heidelberg, INF 350, D-69120 Heidelberg, Germany. E-mail address: brigitte.wildemann@med.uni-heidelberg.de

The online version of this article contains supplemental material.

Abbreviations used in this article: CIS, clinically isolated syndrome suggestive of multiple sclerosis; HC, healthy control donor; MS, multiple sclerosis; Tcon, conventional T cell; Treg, regulatory T cell.

previously that homeostatic changes in the Treg compartment affect total Treg function (3–5), Tregs were further separated according to surface expression of CD45RA in naive and memory Treg subtypes. We used this experimental approach to screen for differences in the mode of suppression between cells isolated from peripheral blood of healthy donors versus those obtained from MS patients. The recorded Ca^{2+} signaling components were correlated with the subordinate nuclear translocation of NFAT that propagates the Ca^{2+} signal to the nucleus to initiate gene transcription, as, for example, for IFN-γ or IL-2 (12). These readouts were complemented by assessing proliferative responses and cytokine release of TCR-triggered Tcons.

Materials and Methods

Human samples

Peripheral blood samples (40–50 ml) were obtained from 19 healthy control donors [(HC), mean age: 33.6 y; range: 21–55 y] and from 13 patients with relapsing-remitting MS ($n = 9$) or a clinically isolated syndrome suggestive of MS [(CIS), $n = 4$] according to the revised McDonald criteria (13): means of age, 35.1 y (range: 22–56 y); previous relapses, 1.8 (range: 1–6); mean Expanded Disability Status Scale, 2.7 (range: 0–6.5); and disease duration range, 1–5 y. Ten patients had clinically active disease, and three patients were in clinical remission. None of the patients had been treated with corticosteroids within ≥ 3 mo prior to the time of blood sampling or had received immunomodulatory agents in the past. The protocol was approved by the University Hospital Heidelberg ethics committee, and all individuals gave written informed consent.

Cells

PBMCs were isolated by density-gradient centrifugation with Ficoll-Hypaque (Biochrom AG, Berlin, Germany). Tregs were isolated using a Regulatory $CD4^+CD25^+$ T Cell Kit (Invitrogen). The remaining Treg-depleted PBMCs were retained and, if required, Tcons were additionally isolated from PBMCs by a $CD4^+$ T Cell Negative Isolation Kit (Invitrogen). Prestimulated Tregs or Tcons were induced with soluble anti-CD3 (1 μg/ml, clone OKT3; eBioscience) and anti-CD28 (0.5 μg/ml, clone CD28.2; eBioscience) mAbs, followed by 24 h of incubation at 37°C and 5% CO_2 in 96-well plates in 200 μl culture medium (RPMI 1640, supplemented with penicillin–streptomycin and 5% FCS). The same conditions were chosen for coculture experiments with 24 h of incubation of Tregs and PBMCs (ratio: 1:2). For calcium imaging, cells were loaded with Fura-2 AM (Invitrogen) in culture medium (supplemented with HEPES) at room temperature for 25 min and washed with fresh medium. Cells were either immediately used or stored at 4°C for ≤ 3 h.

Live-cell imaging

In coculture assays with prestimulated Tregs, IL-2 and IFN-γ mRNA production in Tcons is considerably suppressed already within hours after TCR stimulation (14). As IL-2 and IFN-γ transcription critically depends on the effectual activation of the preceding Ca^{2+}/NFAT pathway, we established a live-cell imaging protocol to determine the impact of prestimulated Tregs on Ca^{2+} signaling and subordinate nuclear translocation of NFAT in Tcons. The setting of the live-cell imaging system is schematically shown in Supplemental Fig. 1.

With this setup, isolated Tregs can be reunited with PBMCs or Tcons on site. Tregs that had been prestimulated for 24 h with anti-CD3 and anti-CD28 mAbs were allowed to adhere to a poly-L-lysine–coated (0.1 mg/ml; Sigma-Aldrich) glass coverslip at room temperature in a sandwiched, self-made chamber, which permits solution exchanges within < 1 s. Subsequently, PBMCs or Tcons were inserted into the chamber; they descended to the bottom and occupied the interspace between Tregs, thereby forming random cell–cell contacts (Supplemental Fig. 2, Supplemental Video 1, Supplemental Video 2). Excess nonadherent cells were removed by a single flush with buffer solution after 6 min. TCR triggering with anti-CD3 mAb followed 2 min later. The measurement chamber was then placed on a Nikon Eclipse Ti inverted microscope equipped with a 20× S Fluor objective (numerical aperture: 0.75) and additional 1.5× intermediate enlargement, resulting in a 30× optical magnification. Experiments were performed in HBSS medium with Ca^{2+} and Mg^{2+}, but no phenol red (Life Technologies), and supplemented with 0.1% FCS (PAA) and reduced L-glutathione, 1 mg/l (Roth). Cells were alternately illuminated (Intensilight; Nikon) at 340 nm and 387 nm with an automatic filter wheel exchanger (Λ 10-2; Sutter). The emission signals at 468–550 nm were recorded with a charge-coupled device camera (ORCA-AG, Hamamatsu). Data collection was controlled by NIS-Elements 3.0 software (Nikon). Ratio images were recorded at intervals of 10 s. Single-cell Ca^{2+} signals were obtained by manually inserting regions of interest into the recorded imaging experiment. Calcium influx $[Ca^{2+}]_i$ was calculated according to the relation $[Ca^{2+}]_i = K^* (R - R_{min})/(R_{max} - R)$, where the values of K^*, R_{min}, and R_{max} were determined by calibrating the setup with Fura-2 pentapotassium salt (Invitrogen) and calcium buffers (Invitrogen). Fig. 1 shows the different readouts of calcium influx that were calculated for each imaging experiment: maximum peak level = $[Ca^{2+}]_{max}$, area under the curve = $[Ca^{2+}]_{auc}$, number of oscillations = $[Ca^{2+}]_{osc}$, and cumulative duration of oscillations = $[Ca^{2+}]_{t\text{-}osc}$.

Classification of cell populations and NFAT localization

To classify the different cell populations and the subcellular distribution of NFAT, cells were immediately fixed (Fixation & Permeabilization Buffer; eBioscience) on the microscope stage after the experiment, permeabilized, and stained with fluorescent mAbs obtained from BD Pharmingen (anti–human CD3 Pacific blue, anti–human CD4 PerCP), Dako (anti–human CD25, PE), eBioscience (anti–human FOXP3-AF647), Santa Cruz Biotechnology (anti–human NFATc1-AF488), and BD Pharmingen (CD45RA APC-H7). Nuclei were stained with DAPI (Sigma-Aldrich). For epifluorescence, microscopy standard filter sets (AHF; Analysetechnik) were used (Supplemental Fig. 3).

Cytokine assays

To assess cytokine production, PBMCs or Tcons were stimulated in culture medium (RPMI 1640 medium, supplemented with penicillin–streptomycin and 5% FCS) with anti-CD3/CD28 mAbs in the live-cell imaging measurement chamber either alone or in the presence of Tregs (ratio 1:1). The supernatants were retained by exchanging the chamber solution and analyzed by ELISA (R&D Systems Europe).

Proliferation assays

In vitro proliferation assays were performed as previously described (3, 5). In brief, 10^5 freshly isolated Tcons were incubated alone or in coculture with 2.5×10^4 Tregs (ratio: 4:1) and polyclonally activated by adding soluble anti-CD3 (1 μg/ml) and anti-CD28 mAbs (1 μg/ml). After 4 d, cells were pulsed for 16 h with 1 μCi [^{3}H]-thymidine per well. After harvesting, T cell proliferation was measured with a scintillation counter.

Flow cytometry

Treg and Tcon subtypes were identified and quantified using multicolor flow cytometry after surface staining of PBMCs with mAbs specific for CD4, CD25, CD127, CD45RA, and CD31 and intracellular staining for FOXP3, as previously described (3, 5).

Data analysis

For data analysis, single-cell signals were extracted from the raw data with NIS-Elements AR (Nikon). Data were processed to determine characteristic signaling patterns individually, using Igor Pro (WaveMetrics). Statistical analysis was performed with Excel (Microsoft) and IBM SPSS Statistics software, version 20.0 (SPSS, Chicago, IL). A nonparametric test (two-tailed Mann–Whitney U test) was applied for statistical analysis of Ca^{2+} data. Fisher's exact test was used to examine the significance of categorical data. A p value <0.05 was considered significant.

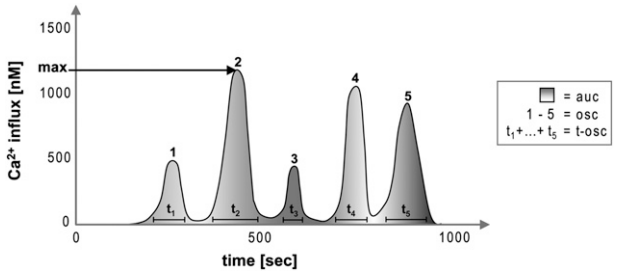

FIGURE 1. Readouts of Ca^{2+} signaling. The recorded calcium influx of a single Tcon following TCR triggering obtained by live-cell imaging is shown schematically. auc, Area under the curve = total calcium influx; max, maximum peak level of Ca^{2+} influx; osc, number of Ca^{2+} peaks; t-osc, cumulative duration of oscillations.

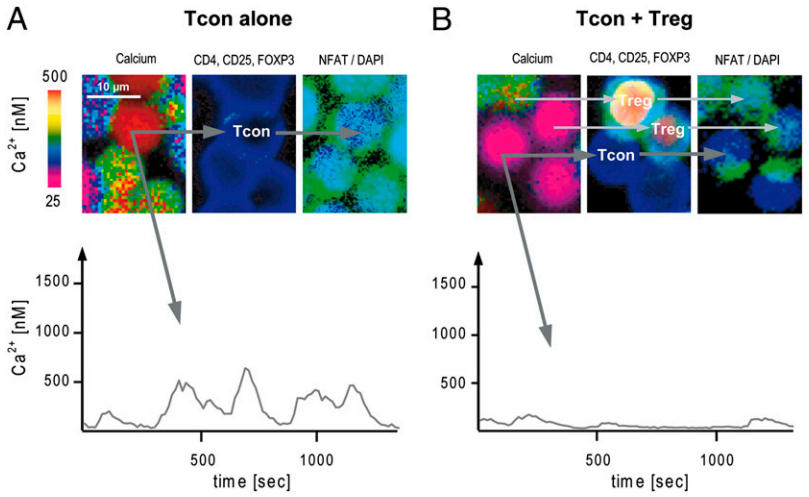

FIGURE 2. Single-cell Ca^{2+} imaging in classified T cells. Direct cell contact with Tregs suppresses the occurrence of Ca^{2+} signals in Tcons. Live-imaging pictures and corresponding single-cell Ca^{2+} signals of one TCR-triggered Tcon without (**A**) or with (**B**) direct cell–cell contact with one Treg. *Upper row, left panels*, Color-coded details of ongoing calcium imaging experiments at a single measurement point. Warmer colors (yellow/red) indicate high $[Ca^{2+}]_i$, whereas colder colors (blue/pink) indicate low $[Ca^{2+}]_i$. *Upper row, central panels*, Corresponding image sections with fixed and stained cells after live-cell imaging: red, anti-FOXP3; blue, anti-CD4; green, anti-CD25. *Upper row, right panels*, Staining with anti-NFAT (green) and counterstaining of the nuclei with DAPI. An overlay of NFAT and DAPI signals indicates nuclear translocation of NFAT. The corresponding kinetics of Tcon Ca^{2+} influx are given in the *lower row*.

Results

Tregs rapidly reduce Ca^{2+} influx and downstream signals in Tcons upon cell contact

We used single-cell live imaging to analyze the influence of Tregs on cell contact–dependent Ca^{2+} signaling in Tcons (Fig. 1). Tcons derived from HC (n = 11) were TCR triggered in the presence of prestimulated syngeneic Tregs (2:1 ratio), and Ca^{2+} influx was comparatively assessed in individual Tcons with (n = 361) or without (n = 499) close contact with Tregs (as defined by overlapping CD4 surface-staining signals). We found that intimate contact with Tregs was essential to suppress Ca^{2+} signaling and Ca^{2+}-driven nuclear import of NFAT in Tcons. In contrast, calcium signaling was either not downregulated ($[Ca^{2+}]_{max}$, $[Ca^{2+}]_{auc}$) or only marginally downregulated ($[Ca^{2+}]_{osc}$, $[Ca^{2+}]_{t\text{-}osc}$) in Tcons that did not have direct contact with Tregs (as shown, for example, in Fig. 2; data given in Fig. 3).

Ca^{2+} signals in Tcons not having contact with Tregs did not significantly differ from Tcons that were stimulated in the absence of Tregs. We did not observe any effects on Ca^{2+} signals when Tcons were TCR triggered in the presence of non-prestimulated Tregs or if prestimulated Tcons were used instead of prestimulated Tregs (not depicted).

We next aimed to verify whether the experimental conditions were appropriate for inhibiting functional consequences of T cell activation. PBMCs were TCR stimulated alone or in the presence of HC Tregs (n = 4). Tregs efficiently suppressed IL-2 and IFN-γ (Fig. 3C) production by Tcons as early as 24 h after stimulation, as determined by serial assessment of suppression supernatants.

Both Treg-mediated inhibition of Tcon Ca^{2+} signaling and calcium influx in Tregs upon TCR triggering are reduced in MS

To test the hypothesis that the functional Treg defect in MS is linked to an impaired interference with Ca^{2+} signaling in target

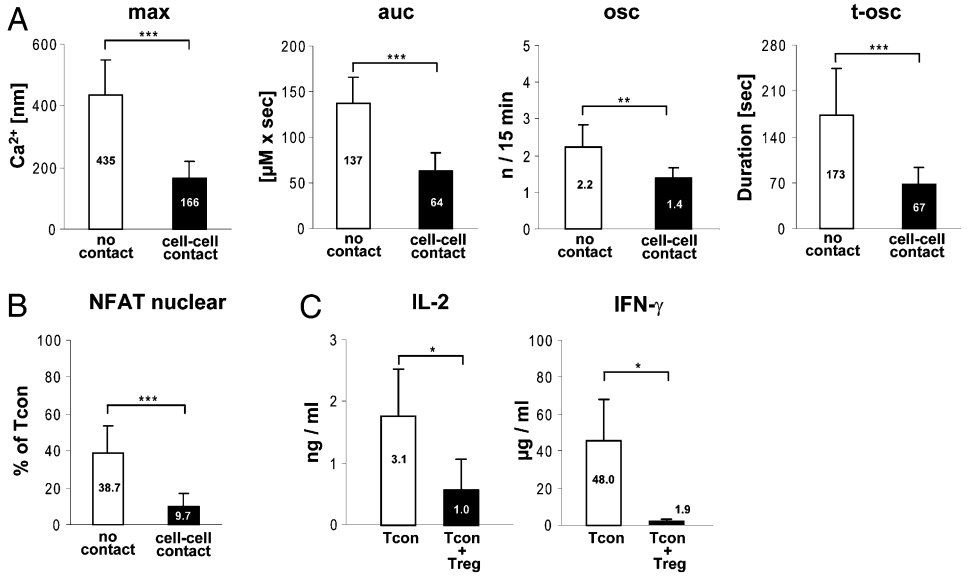

FIGURE 3. Tregs rapidly reduce Ca^{2+} influx and downstream signals in Tcons upon cell contact. Primary readouts of Ca^{2+} signaling (**A**) and NFAT activation (**B**) in TCR-triggered Tcons with (n = 361; filled bars) or without (n = 499; white bars) contact with prestimulated syngeneic Tregs (2:1 ratio; n = 11 independent experiments, n = 6 HCs) and Ca^{2+} signals were recorded without any additional interventions. Histograms illustrate mean values ± SD. Only direct contact with Tregs results in a markedly reduced calcium influx and nuclear transportation of NFAT in Tcons. (**C**) Tregs effectively inhibit secretion of IL-2 and IFN-γ within the first 24 h of coculture. Tcons were kept in the measurement chamber and were stimulated with anti-CD3/CD28 mAbs alone or in the presence of Tregs (ratio 1:1), and supernatants were assessed by ELISA. Data represent mean values from three independent sets of experiments. *$p < 0.05$, **$p < 0.01$, ***$p < 0.001$.

Tcons, we used single Tcons and Tregs obtained from MS patients (n = 9) and HCs (n = 9) to determine whether cell contact–dependent Ca^{2+} influx was reduced in Tcons. In total, 1539 cell clusters composed of one single Treg and one to six surrounding Tcons were assessed. On average, HC-derived Tregs downregulated the maximum Ca^{2+} influx in the sum of Tcons recorded by 61.9 ± 23.4%. When using cells from MS patients, the mean suppression of $[Ca^{2+}]_{max}$ mediated by Tregs was clearly reduced (38.0 ± 15.4%, p = 0.02; Fig. 4A).

To elucidate this difference in more detail, we next determined the number of Tcons that were suppressed by a single Treg. A single Tcon was classified as "suppressed" when its maximum Ca^{2+} influx was reduced by ≥ 15% upon forming cell contact with one Treg. When using HC-derived cells, almost three fourths (72.6 ± 4.7%) of Tcons displaying close contact with the index Treg became rapidly suppressed (Fig. 4B), thereby demonstrating the ability of Tregs to simultaneously inhibit more than one target cell at the same time. The number of adjacent Tcons per single Treg had no impact on Treg inhibition rates and did not differ between study cohorts (HC: mean, 2.8 ± 0.6 Tcons per Treg; MS: mean, 3.2 ± 0.5 Tcons per Treg; p = 0.23). Strikingly, MS Tregs suppressed significantly fewer surrounding Tcons, and a reduction in $[Ca^{2+}]_{max}$ could be detected only in 63.8 ± 10.3% Tcons (p = 0.04; Fig. 4B). Notably, a small contingent of Tregs completely failed to reduce $[Ca^{2+}]_{max}$ in any surrounding Tcons, and this fraction of "nonsuppressors" was significantly higher among MS Tregs (mean: 24.4 ± 11.8%) than HC Tregs (mean: 13.6 ± 5.1%; p = 0.05; Fig. 4C). As a contrasting observation, half of HC Tregs (53.0 ± 8.7%), but only 31.6 ± 13.7% of MS Tregs, categorically diminished $[Ca^{2+}]_{max}$ in every adjacent Tcon (p = 0.02). When percentages of "nonsuppressors" were plotted against the percentages of mean $[Ca^{2+}]_{max}$ obtained from intraindividual Tcons, we found a clear, negative correlation between overall Treg suppressive capacities and the prevalence of "nonsuppressors" (r^2 = 0.44; Fig. 4D).

To compare activation-induced Ca^{2+} influx in Tregs and Tcons from the two study cohorts, we separately assessed monocultures of TCR-triggered Tregs (n = 600) and Tcons (n = 800) (obtained from 9 MS patients, 4 CIS patients, and 13 HCs). We found that Ca^{2+} signals were significantly downscaled in MS Tregs, whereas the difference in Tcon Ca^{2+} signaling between study groups was not significant (Fig. 4E).

Parallel data from in vitro proliferation assays and live imaging of single cells obtained from the same donor were available from six patients and six HCs. As expected, HC Tregs suppressed the proliferative immune responses of Tcons much better than did MS Tregs (Fig. 4F).

$CD45RA^+$ naive Tregs exhibit superior suppressive capacities compared with memory Tregs and are reduced in MS

We next determined inhibitory potencies of naive and memory Treg subtypes at the single-cell level. We assessed Ca^{2+} signaling patterns, together with intracellular expression of FOXP3 and surface expression of CD4, CD25, and CD45RA, in 555 individual

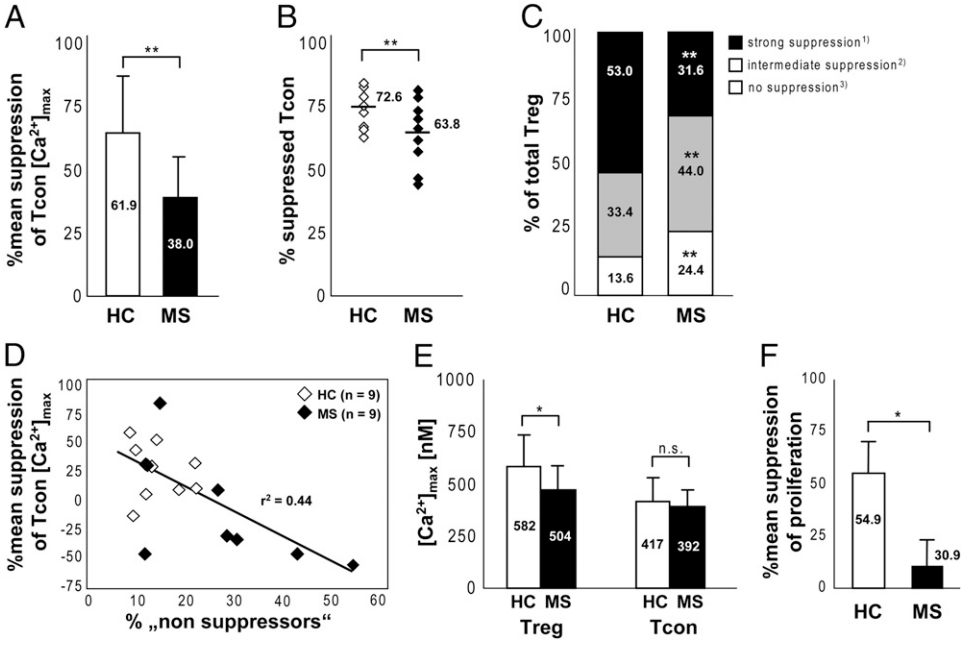

FIGURE 4. Both Treg-mediated inhibition of Tcon Ca^{2+} signaling and activation-induced calcium influx in Tregs are reduced in MS. Single-cell analysis of Treg-mediated suppression of $[Ca^{2+}]_{max}$ in Tcons. A total of 824 (n = 9 MS) and 715 (n = 9 HC) cell clusters composed of one single Treg and one to six surrounding Tcons was assessed. (**A**) Bars represent mean Treg-mediated suppression of $[Ca^{2+}]_{max}$ in the sum of Tcons recorded. When using cells from MS patients, the mean suppression rate was clearly reduced compared with that in HC-derived cells. (**B**) The numbers of Tcons suppressed by cell contact with Tregs are significantly reduced in MS: In the presence of patient-derived Tregs, significantly fewer Tcons show inhibition of $[Ca^{2+}]_{max}$ (Tcons were classified as "suppressed" when $[Ca^{2+}]_{max}$ was reduced by 15–100% upon forming cell contact with a single Treg). (**C**) The fraction of Tregs provoking no (<1%) reduction in $[Ca^{2+}]_{max}$ in surrounding Tcons ("nonsuppressors") is elevated among patient-derived Tregs. [1)]Strong suppression, Downregulation of Ca^{2+} influx in 100% of adjacent Tcons; [2)]Intermediate suppression, Downregulation of Ca^{2+} influx in 17–83% of adjacent Tcons; [3)]No suppression, Downregulation of Ca^{2+} influx in 0% of adjacent Tcons. (**D**) When percentages of "nonsuppressors" were plotted against percentages of mean $[Ca^{2+}]_{max}$ obtained from intraindividual Tcons, we found a clear negative correlation between overall Treg suppressive capacities and the prevalence of "nonsuppressors." (**E**) Means ± SD of maximum Ca^{2+} influx in separately assessed monocultures of TCR-triggered Tregs (n = 600) and Tcons (n = 800) (obtained from 9 MS, 4 CIS, and 13 HCs). $[Ca^{2+}]_{max}$ is significantly downscaled in MS Tregs versus HC Tregs. The difference in Tcon Ca^{2+} signaling between study groups was not significant. (**F**) Parallel data from in vitro proliferation assays (n = 6 MS, n = 6 HCs). As expected, MS Tregs provoke a significantly lower inhibition of Tcon proliferation than do HC Tregs. Histograms illustrate mean values ± SD. *$p < 0.05$. **$p < 0.01$.

Tregs (obtained from five HCs and five patients). We found that $CD4^+CD25^+FOXP3^+CD45RA^+$ Tregs suppressed significantly more adjacent Tcons than did $CD4^+CD25^+FOXP3^+CD45RA^-$ memory Tregs (74.5 ± 21.1% versus 62.0 ± 25.3%; $p < 0.001$; Fig. 5A). Of note, nonsuppressive cells were exclusively present in the memory fraction, whereas three fourths of cells in the naive fraction showed high suppressive activity, with 50–100% suppressed Tcons (Fig. 5B). As another prominent feature, Ca^{2+} signatures recorded in TCR-triggered naive Tregs revealed considerably higher values of Ca^{2+} influx than did those in memory Tregs (Fig. 5C). Furthermore, naive Tregs exhibited lower FOXP3 expression levels than did Tregs harboring a $CD45RA^-$ memory phenotype (Fig. 5D). Whether memory Tregs or naive Tregs were obtained from HC donors or MS patients had no influence on individual suppressive capacities, calcium signatures, or FOXP3 expression levels. In contrast, MS Tregs showed markedly lower numbers of $CD45RA^+$ cells than did HC Tregs (HC: 37.1 ± 9.2% versus MS: 25.3 ± 11.9%; $p < 0.05$; Fig. 5E). This finding was confirmed by parallel flow cytometric data (available from eight patients and six HCs), revealing reduced frequencies of $CD45RA^+$ naive and $CD31^+CD45RA^+$ recent thymic emigrant cells among circulating MS Tregs (naive Tregs: MS, 26.7 ± 10.4%, versus HC, 34.0 ± 6.6%, $p = 0.01$; recent thymic emigrant Tregs: MS, 2.6 ± 1.9%, versus HC, 4.9 ± 2.8%; $p = 0.04$).

Discussion

We hypothesized that interference with Ca^{2+} signaling in Tcons as a pivotal mechanism used by Tregs to confer suppression of Tcon activation might differ among Treg subsets and might contribute to the Treg defect that has been reported for MS and other autoimmune diseases (15). Our data show that normal human Tregs rapidly reduced TCR-triggered Ca^{2+} signaling and activation of NFAT in Tcons, thereby prompting the inhibition of Tcon immune activity, as reflected by substantially diminished IL-2 and IFN-γ release and dampened proliferation. These findings are well in line with the results of a recent study that used cocultured, purified T cell populations instead of single cells to demonstrate rapid suppression of Tcon Ca^{2+} signaling by Tregs, followed by downregulation of NFAT1 and NF-κB (11). The fast kinetics of cytokine suppression observed in our study is also consistent with the results of a previous study showing that Tregs inhibit the induction of Th1 cytokine mRNA in Tcons as early as 1 h after TCR activation (14). Calcium influx suppression was most pronounced when Tcons were in close contact with Tregs, supporting the model of contact dependency that was originally deduced from proliferation assays (16, 17) and reinforced by the more recent demonstration of gap junction formation between Tregs and Tcons (18).

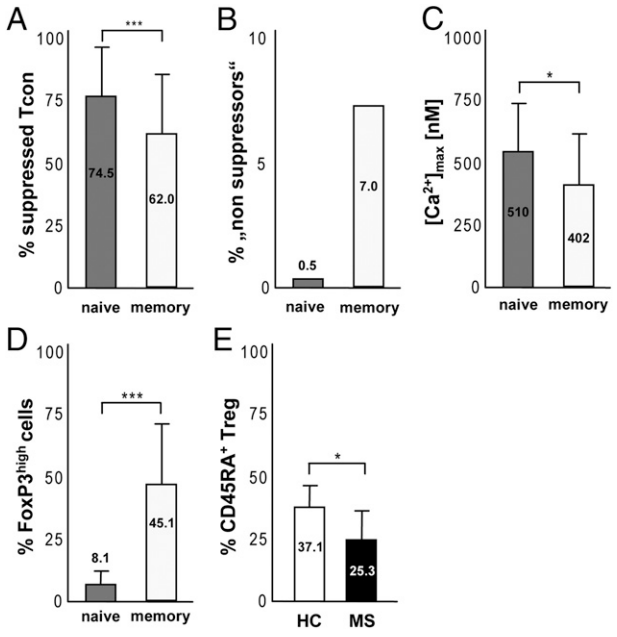

FIGURE 5. $CD45RA^+$ naive Tregs exhibit superior suppressive capacities and heightened Ca^{2+} influx upon TCR triggering, compared with memory Tregs, and are reduced in MS. Single-cell analysis of suppression of $[Ca^{2+}]_{max}$ in Tcons, calcium influx, and FOXP3 expression levels in 555 Tregs obtained from five HCs and five MS patients, subdivided into $CD4^+CD25^+FOXP3^+CD45RA^+$ naive and $CD4^+CD25^+FOXP3^+CD45RA^-$ memory subsets. (**A**) Naive Tregs suppress significantly more adjacent Tcons than do memory Tregs. (**B**) Nonsuppressive cells are exclusively present in the memory fraction of both cohorts, whereas $CD45RA^+$ Tregs consist of >75% highly suppressive cells. (**C**) TCR-triggered naive Tregs reveal considerably higher values of $[Ca^{2+}]_{max}$ and $[Ca^{2+}]_{auc}$ than do memory Tregs. (**D**) Naive Tregs contain lower numbers of $FOXP3^{high}$ cells than do memory Tregs. (**E**) Tregs obtained from MS patients contain significantly fewer naive Tregs than do those from HCs. *$p < 0.05$, ***$p < 0.001$. Histograms illustrate mean values ± SD.

Next, we comparatively assessed the impact of Tregs on Tcon Ca^{2+} signaling, using cells derived from HCs and from MS patients to elucidate in more detail how Tregs confer suppression at the single-cell level. Notably, although Tregs consistently prompted downregulation of Ca^{2+} influx in the large majority of neighboring Tcons in the HC group, the number of Tcons exhibiting a clear decrease in Ca^{2+} signals when located in direct cell contact with a single Treg was significantly decreased in MS, thus explaining the diminished performance of MS Tregs to downregulate mean calcium signals recorded from Tcons. This finding was paralleled by a marked increase in the percentage of cells among patient-derived Tregs that completely failed to suppress Ca^{2+} signaling in adjacent Tcons. These abnormalities are in line with an earlier report demonstrating that only a minority of Treg clones derived from MS patients exhibit regulatory activity (19). That and other previous studies have shown that the reduced inhibitory capacity of Tregs in MS is based on a defective performance of Treg or Treg subsets (7), and these investigations did not find evidence of an abnormal resistance of Tcons toward Treg-mediated suppressive signals (19–21). In line with this knowledge, we did not detect a higher activation state of TCR-triggered MS Tcons with respect to Ca^{2+} influx in single cells and proliferation. Thus, our data show that loss of inhibitory function in MS is not evenly distributed within the Treg population as a whole.

When we screened for distinguishing features between suppressive and nonsuppressive cells, we found that $CD45RA^+$ naive cells were enriched in the fraction of Tregs classified as strongly suppressive. Consistent with the reduced proportions of strongly suppressive cells, MS-derived Tregs contained significantly fewer naive cells than did HC Tregs, which is well in line with earlier reports on disturbed T cell and Treg homeostasis in MS (3–5, 9, 10, 22, 23). Naive Tregs featured lower FOXP3 expression, a finding that is corroborated by a previous study (24) and, as a highly important distinctive property, diverged from memory counterparts with regard to the Ca^{2+} signature evoked after TCR triggering. Naive subtypes derived from both HC donors and MS patients consistently featured a considerably heightened Ca^{2+} influx upon activation. This characteristic coincided with a superior potency to counteract sustained elevation of calcium in Tcons and directly correlated with higher proportions of adjacent Tcons becoming efficiently suppressed compared with memory Tregs. In line with these observations, nonsuppressive cells were exclusively detected in the memory Treg subset. Thus, the activation-induced increase in Ca^{2+} influx, as revealed in this study, appears to reflect a higher reactivity of naive Tregs and suggests a more

sustained functional fitness of this subtype. In agreement with this hypothesis, naive Tregs, unlike memory Tregs, are insensitive to apoptotic elimination, remain proliferative ex vivo, and maintain full inhibitory activity after expansion (24–26).

Taken together, our data support the idea that average, Treg-mediated suppression rates, as measured by conventional in vitro proliferation assays, directly depend on the numbers of suppressed Tcons, which in turn are determined by the prevalence of highly suppressive naive Tregs. Consequently, the homeostatic imbalance in the peripheral Treg compartment in patients with MS, as described previously (3–5), is sufficient to explain the Treg defect associated with this condition because the contraction in naive and recent thymic emigrant subtypes and the concomitant shift toward functionally exhausted memory cells containing high numbers of "nonsuppressors" obviously cannot sustain the full inhibitory capacity of total Tregs. This model also explains the physiological decline in Treg inhibitory activity in elderly persons (3). The insights gained from this study might apply to numerous other autoimmune disorders and support efforts to therapeutically strengthen the compromised activity of Tregs in human autoimmunity.

Acknowledgments

We thank the patients and healthy donors for participation in this study; Brigitte Fritz for outstanding technical assistance; and the Nikon Imaging Center at the University of Heidelberg for the live-cell imaging setup.

Disclosures

The authors have no financial conflicts of interest.

References

1. Wing, K., and S. Sakaguchi. 2010. Regulatory T cells exert checks and balances on self tolerance and autoimmunity. *Nat. Immunol.* 11: 7–13.
2. Zozulya, A. L., and H. Wiendl. 2008. The role of regulatory T cells in multiple sclerosis. *Nat. Clin. Pract. Neurol.* 4: 384–398.
3. Haas, J., B. Fritzsching, P. Trübswetter, M. Korporal, L. Milkova, B. Fritz, D. Vobis, P. H. Krammer, E. Suri-Payer, and B. Wildemann. 2007. Prevalence of newly generated naive regulatory T cells (Treg) is critical for Treg suppressive function and determines Treg dysfunction in multiple sclerosis. *J. Immunol.* 179: 1322–1330.
4. Venken, K., N. Hellings, T. Broekmans, K. Hensen, J. L. Rummens, and P. Stinissen. 2008. Natural naive CD4+CD25+CD127low regulatory T cell (Treg) development and function are disturbed in multiple sclerosis patients: recovery of memory Treg homeostasis during disease progression. *J. Immunol.* 180: 6411–6420.
5. Haas, J., M. Korporal, A. Schwarz, B. Balint, and B. Wildemann. 2011. The interleukin-7 receptor α chain contributes to altered homeostasis of regulatory T cells in multiple sclerosis. *Eur. J. Immunol.* 41: 845–853.
6. Lowther, D. E., and D. A. Hafler. 2012. Regulatory T cells in the central nervous system. *Immunol. Rev.* 248: 156–169.
7. Dominguez-Villar, M., C. M. Baecher-Allan, and D. A. Hafler. 2011. Identification of T helper type 1-like, Foxp3+ regulatory T cells in human autoimmune disease. *Nat. Med.* 17: 673–675.
8. Baecher-Allan, C. M., C. M. Costantino, G. L. Cvetanovich, C. W. Ashley, G. Beriou, M. Dominguez-Villar, and D. A. Hafler. 2011. CD2 costimulation reveals defective activity by human CD4+CD25(hi) regulatory cells in patients with multiple sclerosis. *J. Immunol.* 186: 3317–3326.
9. Korporal, M., J. Haas, B. Balint, B. Fritzsching, A. Schwarz, S. Moeller, B. Fritz, E. Suri-Payer, and B. Wildemann. 2008. Interferon beta-induced restoration of regulatory T-cell function in multiple sclerosis is prompted by an increase in newly generated naive regulatory T cells. *Arch. Neurol.* 65: 1434–1439.
10. Haas, J., M. Korporal, B. Balint, B. Fritzsching, A. Schwarz, and B. Wildemann. 2009. Glatiramer acetate improves regulatory T-cell function by expansion of naive CD4(+)CD25(+)FOXP3(+)CD31(+) T-cells in patients with multiple sclerosis. *J. Neuroimmunol.* 216: 113–117.
11. Schmidt, A., N. Oberle, E. M. Weiss, D. Vobis, S. Frischbutter, R. Baumgrass, C. S. Falk, M. Haag, B. Brügger, H. Lin, et al. 2011. Human regulatory T cells rapidly suppress T cell receptor-induced Ca(2+), NF-κB, and NFAT signaling in conventional T cells. *Sci. Signal.* 4: ra90.
12. Rao, A., C. Luo, and P. G. Hogan. 1997. Transcription factors of the NFAT family: regulation and function. *Annu. Rev. Immunol.* 15: 707–747.
13. Polman, C. H., S. C. Reingold, G. Edan, M. Filippi, H. P. Hartung, L. Kappos, F. D. Lublin, L. M. Metz, H. F. McFarland, P. W. O'Connor, et al. 2005. Diagnostic criteria for multiple sclerosis: 2005 revisions to the "McDonald Criteria." *Ann. Neurol.* 58: 840–846.
14. Oberle, N., N. Eberhardt, C. S. Falk, P. H. Krammer, and E. Suri-Payer. 2007. Rapid suppression of cytokine transcription in human CD4+CD25 T cells by CD4+Foxp3+ regulatory T cells: independence of IL-2 consumption, TGF-beta, and various inhibitors of TCR signaling. *J. Immunol.* 179: 3578–3587.
15. Brusko, T. M., A. L. Putnam, and J. A. Bluestone. 2008. Human regulatory T cells: role in autoimmune disease and therapeutic opportunities. *Immunol. Rev.* 223: 371–390.
16. Takahashi, T., Y. Kuniyasu, M. Toda, N. Sakaguchi, M. Itoh, M. Iwata, J. Shimizu, and S. Sakaguchi. 1998. Immunologic self-tolerance maintained by CD25+CD4+ naturally anergic and suppressive T cells: induction of autoimmune disease by breaking their anergic/suppressive state. *Int. Immunol.* 10: 1969–1980.
17. Thornton, A. M., and E. M. Shevach. 1998. CD4+CD25+ immunoregulatory T cells suppress polyclonal T cell activation in vitro by inhibiting interleukin 2 production. *J. Exp. Med.* 188: 287–296.
18. Bopp, T., C. Becker, M. Klein, S. Klein-Hessling, A. Palmetshofer, E. Serfling, V. Heib, M. Becker, J. Kubach, S. Schmitt, et al. 2007. Cyclic adenosine monophosphate is a key component of regulatory T cell-mediated suppression. *J. Exp. Med.* 204: 1303–1310.
19. Viglietta, V., C. Baecher-Allan, H. L. Weiner, and D. A. Hafler. 2004. Loss of functional suppression by CD4+CD25+ regulatory T cells in patients with multiple sclerosis. *J. Exp. Med.* 199: 971–979.
20. Haas, J., A. Hug, A. Viehöver, B. Fritzsching, C. S. Falk, A. Filser, T. Vetter, L. Milkova, M. Korporal, B. Fritz, et al. 2005. Reduced suppressive effect of CD4+CD25high regulatory T cells on the T cell immune response against myelin oligodendrocyte glycoprotein in patients with multiple sclerosis. *Eur. J. Immunol.* 35: 3343–3352.
21. Feger, U., C. Luther, S. Poeschel, A. Melms, E. Tolosa, and H. Wiendl. 2007. Increased frequency of CD4+ CD25+ regulatory T cells in the cerebrospinal fluid but not in the blood of multiple sclerosis patients. *Clin. Exp. Immunol.* 147: 412–418.
22. Hug, A., M. Korporal, I. Schröder, J. Haas, K. Glatz, B. Storch-Hagenlocher, and B. Wildemann. 2003. Thymic export function and T cell homeostasis in patients with relapsing remitting multiple sclerosis. *J. Immunol.* 171: 432–437.
23. Duszczyszyn, D. A., J. L. Williams, H. Mason, Y. Lapierre, J. Antel, and D. G. Haegert. 2010. Thymic involution and proliferative T-cell responses in multiple sclerosis. *J. Neuroimmunol.* 221: 73–80.
24. Fritzsching, B., N. Oberle, E. Pauly, R. Geffers, J. Buer, J. Poschl, P. H. Krammer, O. Linderkamp, and E. Suri-Payer. 2006. Naive regulatory T cells: a novel subpopulation defined by resistance toward CD95L-mediated cell death. *Blood* 108: 3371–3378.
25. Hoffmann, P., R. Eder, T. J. Boeld, K. Doser, B. Piseshka, R. Andreesen, and M. Edinger. 2006. Only the CD45RA+ subpopulation of CD4+CD25high T cells gives rise to homogeneous regulatory T-cell lines upon in vitro expansion. *Blood* 108: 4260–4267.
26. Hoffmann, P., T. J. Boeld, R. Eder, J. Huehn, S. Floess, G. Wieczorek, S. Olek, W. Dietmaier, R. Andreesen, and M. Edinger. 2009. Loss of FOXP3 expression in natural human CD4+CD25+ regulatory T cells upon repetitive in vitro stimulation. *Eur. J. Immunol.* 39: 1088–1097.